

Title	Chiral liquid crystals/TiO ₂ nanocomposites: Enhancement of optical and electrooptical properties
Author(s)	Podgornov, Fedor V.; Haase, Wolfgang; Yoshino, Katsumi
Citation	電気材料技術雑誌. 2011, 20(2), p. 35-42
Version Type	VoR
URL	https://hdl.handle.net/11094/76873
rights	
Note	

Osaka University Knowledge Archive : OUKA

<https://ir.library.osaka-u.ac.jp/>

Osaka University

Chiral liquid crystals/TiO₂nanocomposites: Enhancement of optical and electrooptical properties

Fedor V. Podgornov^{a,b)} and Wolfgang Haase^{a)}

^{a)}Eduard-Zintl-Institute for Inorganic and Physical Chemistry, Darmstadt University of Technology,
Petersenstr. 20, Darmstadt, D-64287, Germany

^{b)}Electrical Engineering Technologies Laboratory, South Ural State University,
Lenin ave., 76, Chelyabinsk, 454080, Russia

Katsumi Yoshino

Shimane Institute for Industrial Technology
1 Hokuryo-cho, Matsue, Shimane 690-0816 Japan

Abstract

The influence of the dielectric TiO₂ nanoparticles on the electrooptical and optical properties of ferroelectric and cholesteric liquid crystals was investigated. It was shown that TiO₂ nanoparticles did not change the tilt angle but further electro optical properties of the Ferroelectric Liquid Crystals like response time, spontaneous polarization, rotational viscosity. Furthermore, these nanoparticles modify the form of the electrooptical response curve due to their influence of the coercive voltage.

It was also demonstrated that dispersing of TiO₂ in Cholesteric Liquid Crystal/dye mixture lead to the significant change of the emission spectra of CLC/DCM/TiO₂ dispersion upon pumping with Nd:YAG laser ($\lambda=532$ nm).

Introduction

Liquid crystals (LCs) are unique materials combining the fluidity of the liquids and the long-range ordering of solid crystals. Currently various liquid crystal phases with different spatial and orientational symmetries are discovered and investigated (1).

Because of the high sensitivity of LCs against external fields (electric, magnetic, temperature and mechanical ones) they are perspective candidates for numerous applications. However, among of all liquid crystal phases, nematic LCs (NLCs) play one of the most important role in modern technologies (2) due to their application in liquid crystal displays (LCDs).

However, in the last years it was demonstrated the incorporation of micro and nanoparticles in LCs lead to new effects as well as enhancement of the physical properties of liquid crystals. It was shown

that particles could induce different topological defects of LC texture which, in turn, promote specific elasticity mediated interactions between constituting particles (3-5). Moreover, novel electrokinetical effects were reported in LCs nanocolloids recently (6,7), which can be utilized for surface sensitive micro and nanoparticles separation and their self-assembling (8). In addition, nanoparticles can change electrooptical, dielectric and nonlinear optical properties of liquid crystals.

For the time being, it was discovered that dispersion of the carbon nanotubes (CNTs), metallic and ferroelectric nanoparticles in nematic liquid crystals enhanced their electrooptical response and modified the dielectric properties. It was shown (9) that due to the ions trapping, doping of NLCs with SWCNT (Single Walled CNTs) or MWCNTs (Multi Walled CNTs)

influences the Freederickz threshold as well as the hysteresis loop which will be reduced under application of dc driving voltage (9,10). In frame of this approach, it was demonstrated that the residual dc voltage in twisted NLCs is greatly suppressed (11). The ion trapping model was also confirmed via transient current measurements (12, 13).

The migration of SiO₂ particles in smectic liquid crystals (14) and the response of silica particles dispersed in liquid crystals under low frequency AC voltage has been described (15).

The reduction of the switching time as well as modification of the dielectric response due to the ions trapping and the shunting of electrical double layers, respectively, were also reported for Ferroelectric LCs (FLCs) doped with SWCNTs and MWCNTs (16, 17).

The influence of the ferroelectric nanoparticles on the dielectric and electrooptical properties of FLCs and NLCs were reported in (18, 19, 20). The dielectric and electrooptical properties of liquid crystals nanodispersions based on gold nanoparticles were reported in series of works (see e.g. 21 and references therein). It was found that the gold nanoparticles influenced the relaxation frequency of both NLC and FLC. In the latter case, the geometrical size of the nanoparticles plays the crucial role in the change of the dielectric strength and relaxation frequency of the Goldstone mode (22).

Nanoparticles can also change the optical properties of chiral liquid crystals. The distinctive property of chiral LCs, particularly Cholesteric Liquid Crystals (CLCs) and FLCs, is their helical structure. The helical pitch can vary from very small values lying in nanometer scale up to infinity in the other extreme. The existence of the helical superstructure leads to selective reflection of the incident electromagnetic irradiation (stop-band zone). The dependence of the helical pitch on the external field leads to (temperature, electric and mechanical field) application of these materials in tunable lasers with distributed feedback or, in

modern interpretation, lasers based on tunable photonic band-gap (PBG) structure.

The latest achievements in this field are summarized in (23). In the same time, nanoparticles can play twofold role in PBG LC lasers. First of all, semiconducting nanoparticles can influence the helical pitch (24, 25) and secondly they can serve as light scattering centers in themirrorless, scattering lasing mode (25). In (25) it was demonstrated that dispersing of TiO₂ nanoparticles in FLCs lead to the appearing of the second lasing peak which was explained by this scattering mode.

The aim of this article is to demonstrate the influence of the TiO₂ nanoparticles on the dielectric and electrooptical properties of FLCs as well as to clarify their role in the lasing of dye doped CLC.

CLC/TiO₂nanodispersion preparation

The cholesteric liquid crystal was prepared using commercially available nematic MLC 2463 and the chiral dopant ZLI -811 (both Merck, Darmstadt). The helical pitch were controlled via the concentration of the chiral component (35 % wt) in such a way that the stop band of CLC was envisaged in the range 532 - 610 nm (between the pumping beam wavelength ($\lambda=532$ nm) and the maximum of the fluorescence spectrum of DCM). The developed CLC was infiltrated in a cell with gap around 20 μ m. The stop band of CLC was measured with the fiber optic spectrometer OceanOptics HR200.

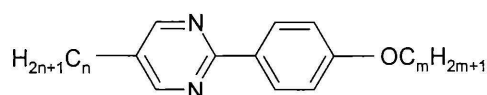
To prepare the CLC nanodispersion, commercially available TiO₂ (Aldrich) particles (average diameter- 100 nm) were dispersed in acetone and sonificated for about 1 hour. The nanoparticles agglomerations were removed with a filter (pores diameter 1 μ m). The concentration of the TiO₂ particles was estimated as 0.1 wt%.

The textures of pure CLC and CLC/TiO₂ were investigated with a polarizing microscope. In case of CLC/TiO₂ dispersion, particles with a diameter of around 800 nm could be observed (the average distance between neighbouring agglomerations was

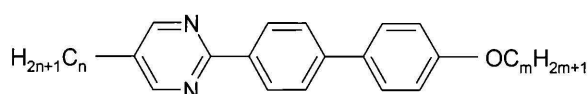
around 10 μ m). The prepared dispersion was doped with DCM, concentration 1.5 wt % and infiltrated in the cell (the cell gap is around 20 μ m) providing homeotropical alignment of CLC.

FLC and FLC/TiO₂ nanodispersion preparation

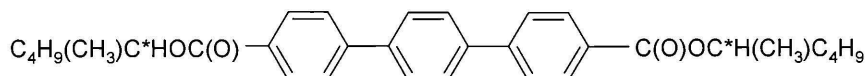
The FLC mixture with the acronym LAH1(26) consists of the following components:



n=8, m=6; n=8, m=8; n=8, m=9



n=8, m=8



The material characteristics and phase sequence are summarized in Table 1

FLC mixture	Phase transitions, °C	Spontaneous polarization Ps, nC/cm ² (T=25°C)	Tilt angle θ° (T=25°C)
LAHS1	Cr <23 SmC* - 69,5-SmA* - 81.1- N* -87.0- I	38	23

Table1: Material parameters of LAHS1: Phase transition SmC*-SmA* are not easy to evaluate; different compared to Ref. 26.

To prepare the FLC/TiO₂ dispersions, the commercially available functionalized TiO₂ nanoparticles with average diameter 100 nm (Aldrich) were dispersed in acetone and sonicated during around 1 hour. To exclude the influence of acetone, the same amount of pure acetone and pure LAHS1 were mixed and after that acetone was removed from both samples by the evaporation at temperature 90°. The absence of acetone was confirmed using NMR and XPS spectroscopic methods. The concentration of TiO₂ in LAHS1 was set to 0.1 wt%. The prepared nanodispersion as well as the pure mixture was confined in the cells with thickness around 2.5 μ m.

The electrooptic parameters (tilt angle, response time, spontaneous polarization and the coercive voltage) of the pure LASH1 and the LAHS1/TiO₂ was measured using a standard electrooptical setup (see e.g.25). The dielectric properties of the investigated samples were investigated with the

impedance analyzer HP4192A in the frequency range 100 Hz – 1MHz.

Lasing in dye doped CLC/TiO₂ nanodispersion.

Experimental setup

The schematic representation of the experimental setup for the investigation of light generation in the CLC/DCM and CLC/DCM/TiO₂ is shown in Fig.1. It consists of a frequency- Q-switched Nd:YAG pulsed laser (wavelength - 532 nm, pulse width - 6 ns, repetition rate - 1 kHz), a photometer to control the intensity of the pumping beam and a fiber-optic spectrometer (spectral resolution – 0.4 nm) to investigate the emitted light. To spatially separate the pumping beam from the emitted one, the samples were inclined at 45°. A pinhole after the laser source controlled the diameter. The intensity of the pumping light was controlled by an attenuator. The Glan prism and the $\lambda/4$ retardation plate transformed the polarization of the laser beam in the

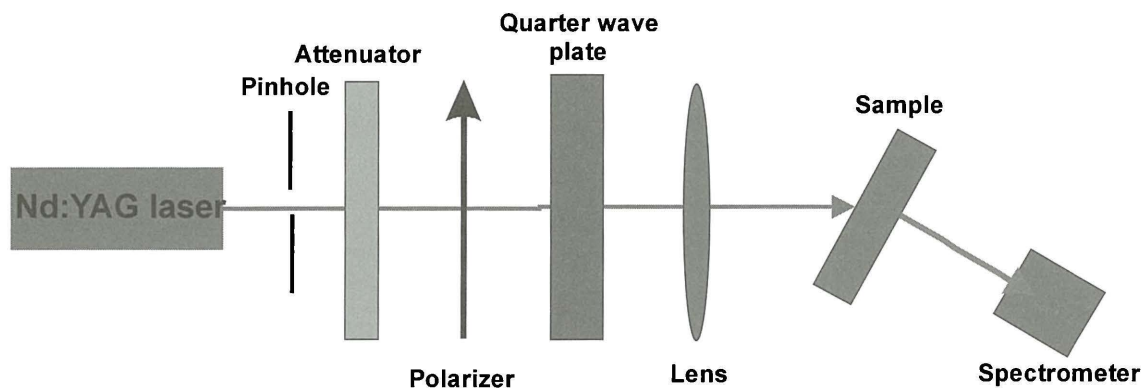


Figure 1: Experimental setup. The pumping beam is incident under an angle of 45° with respect to the cell normal

circular one leading to a counter wise handedness to the CLC helix. The lens focuses the light onto the spot with a diameter of around 200 micrometer.

Experimental results and Discussion

The experimental setup was utilized to investigate the influence of the energy of the pumping beam on the emission spectra of the CLC/DCM and CLC/DCM/TiO₂ samples. To prevent samples from

the heating, the pumping light beam was additionally modulated with a chopper (frequency - 5 Hz). The energy of the pumping pulse varied by the attenuator was from 0.2 $\mu\text{J}/\text{pulse}$ till 10 $\mu\text{J}/\text{pulse}$. The emission spectra of the CLC/DCM cell and nanodispersions are shown in Fig. 2a and Fig. 2 b-d, respectively. The emission line (centered at 576 nm) of the CLC/DCM sample is located at long wavelength edge of the CLC stop band (see Fig. 2a).

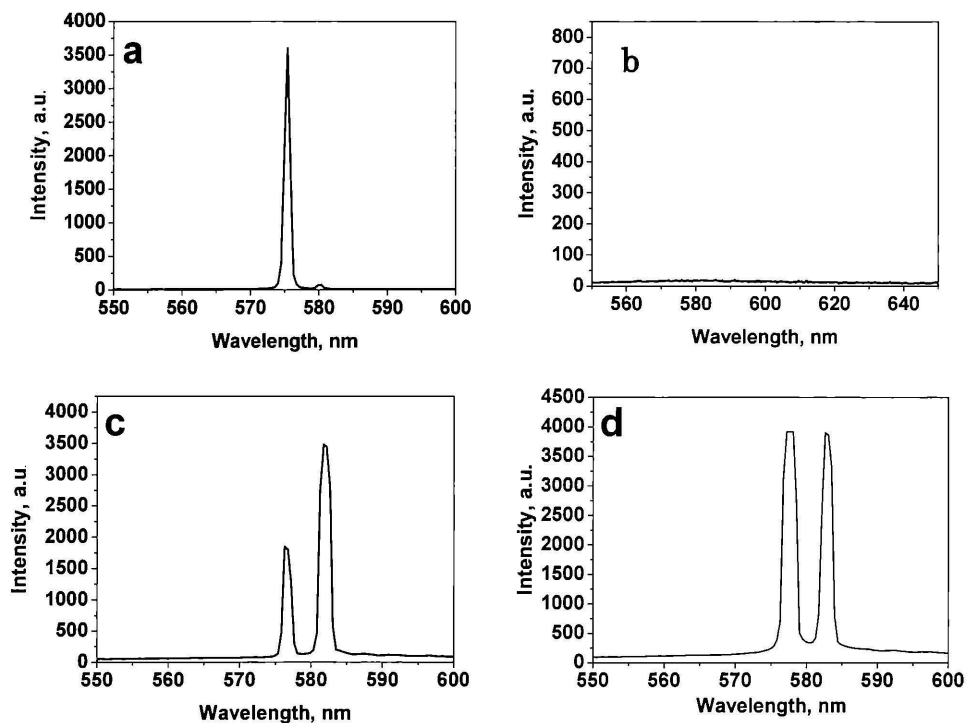


Figure 2: Lasing in CLC/DCM (a) and CLC/DCM/TiO₂(b,c,d) cells. For a) CLC/DCM and b) CLC/DCM/TiO₂ the pumping pulse energy is 3 $\mu\text{J}/\text{pulse}$. c) CLC/DCM/ TiO₂ cell. Pumping energy is 4.5 $\mu\text{J}/\text{pulse}$. d) CLC/DCM/ TiO₂ cell. Pumping energy is 5 $\mu\text{J}/\text{pulse}$. DCM concentration is 1.5 wt.%. Concentration of TiO₂ is 1 wt.%. The diameter of the illuminated area is around 200 μm .

The threshold for the CLC/ DCM/TiO₂ (4.5 μJ/pulse, Fig.2b) is significantly higher than for CLC/DCM (3μJ/pulse, Fig.2a). This difference can be explained by the stronger diffusive light scattering in CLC/DCM/TiO₂. However, the fundamental differences between these samples are the appearing of the second emission peak in the spectrum of the CLC/ DCM/TiO₂ and broadening of these lines in comparison with the emission line of the CLC/ DCM cell.

In our previous publication (25), the origin of the second line was assigned to the lasing due to the light scattering by TiO₂ nanoparticles. But because the concentration of the nanoparticles is rather low, we suggest the other possible mechanisms. One of them is schematically described in Fig. 3b in comparison to that of the undisturbed helix in Fig. 3a. The spatial distribution of the nanoparticles and anchoring of the CLC molecules on their interface can lead to the change of the helical pitch due to its unwinding (in our case it leads to the decrease of the CLC wavevector). As result, in this area of the CLC layer, the emission peak will be shifted towards higher wavelengths. On the output of the cell the emitted light will consist of two components,

those are generated in the regions without nanoparticles and second one coming from the regions with TiO₂ nanoparticles.

The other mechanisms can be explained by the topological defects of the CLC texture induced by the TiO₂ nanoparticles (see Fig. 3c). The homeotropic anchoring of the CLC molecules on the nanoparticles surface will lead to the spatial distribution of the angle orientation of the CLC helix which lead, in turn, to effective increase of the helical pitch (due to the inclination of CLC wavevector with respect to that of the pumping beam). As result, in region near the nanoparticles the wavelength of the emitted light will be shifted towards higher wavelengths. The broadening of the spectral line can be explained, in turn, by the statistical distribution of the helical pitch which results in the spectral shift of the individual emission lines in different parts of the cell.

Influence of TiO₂ nanoparticles on electrooptical switching of Ferroelectric Liquid Crystals.

Results and discussion

The measurements of the tilt angle (θ), spontaneous polarization (P_s) and response time (τ) demonstrated that the response time and the spontaneous polarization of FLC/TiO₂ is lower in comparison with the pure LAHS1 mixture (Fig.4), whereas the tilt angle is practically unaffected by TiO₂ nanoparticles. The simultaneous decrease of the response time and the spontaneous polarization of FLC/TiO₂ nanodispersion can be explained by the growth of the internal electric field most probably due to the partial shunting of the electric double layer at the FLC/polymer alignment layer interface (17, 22), the trapping of the impurity ions by TiO₂ nanoparticles as well as the contribution of the electric field originated from the polarization induced charges in the nanoparticles. In the same time, the decrease of the spontaneous polarization can be assigned to the reduction of the dipole-dipole correlation of FLC molecules as well as

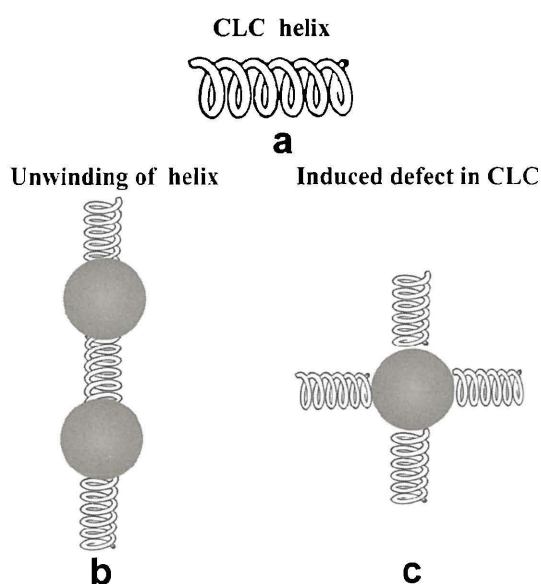


Figure 3 : a) Helical structure of the CLC b) Twist defect of the CLC helix by incorporation of TiO₂ nanoparticles, c) Structural defect of the CLC alignment induced by TiO₂ nanoparticles

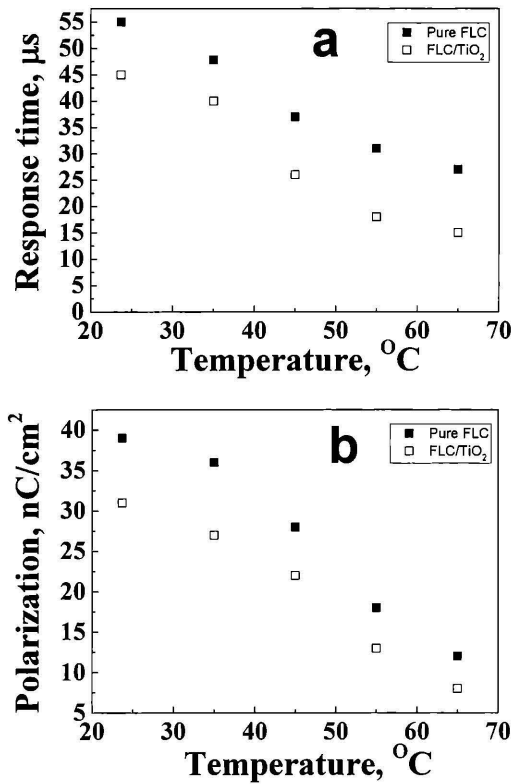


Figure 4: Temperature dependence of response time (a) and spontaneous polarization (b) of pure LAHS1 and LAHS1/ TiO₂nanodispersion.

compensation of the macroscopical dipole moment due to the induced polarization of the nanoparticles.

The investigation of the dielectric properties of LAHS1 and LAHS1/TiO₂ revealed significant influence of TiO₂ on the dielectric strength and the relaxation frequency of Goldstone mode (GM) (Fig.5). The GM relaxation frequency f_G and the dielectric strength of the Goldstone mode $\Delta\epsilon_G$ are related with the material parameters of the FLC through the relations 1 and 2 following from Landau free energy expansion:

$$f_G = K_{33}q^2 / 2\pi\gamma_G \quad 1$$

$$\Delta\epsilon_G = P_s^2 / 2\epsilon_0 \sin^2\theta K_{33}q^2 \quad 2$$

$q = 2\pi/p$ wavevector of the FLC helix (p is the helical pitch), K_{33} is the Frank elastic constant, γ_G is the GM rotational viscosity. However, because the investigated samples are surface stabilized and their helices are unwound, the helical

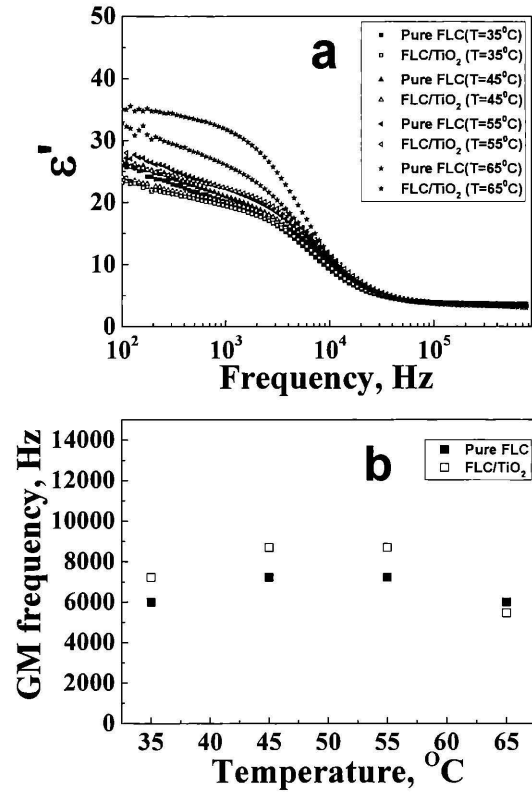


Figure 5: Dependence of the real part of the dielectric constant (a) and the Goldstone mode relaxation frequency (b) on the frequency for pure LAHS1 and LAHS1/TiO₂nanodispersion. Temperatures 35°C, 45°C, 55°C and 65 °C.

pitch for these samples can be taken equal to the cell gap. As one can clearly see from Fig. 5 the GM relaxation frequency of LAHS1/TiO₂ is higher than that of the LAHS1 whereas the dielectric strength is lower in comparison with pure FLC (except the temperature closer to the phase transition $T=65^\circ\text{C}$).

According to the formulae 1 and 2, one of the possible explanations can be the increase of the Frank elastic constant of LAHS1/TiO₂ nanodispersion which, in turn, can be assigned to the growth of the intermolecular interaction energy in FLC due to the presence of nanoparticles.

Modification of the dielectrical and material properties of FLC by TiO₂ nanoparticles leads to the pronounced change of the form of the electrooptical switching. The measurement of the coercive voltage dependence on the frequency of the applied triangular wave electric voltage (amplitude $U=10\text{ V}$, $T=30^\circ\text{C}$) (see Fig. 6) reveals significant increase of

the coercive voltage in the cell with TiO₂ nanoparticles.

The observed effect can be explained by the dynamic voltage divider model proposed in (27, 28, 29). The liquid crystal cell (see its structure Fig.7a) represents a typical voltage divider (see Fig.7b) which characteristics depends on the amplitude and frequency of the applied electric field (27, 28, 29). As it was just demonstrated the incorporation of the TiO₂ nanoparticles in FLC leads to the change of its dielectric properties. Hence, the voltage drops on the liquid crystalline layer will change its value according to the formula (3) deduced for a sinusoidal signal ($U=U_0\sin\omega t$, ω is the angular frequency):

$$U_{LC} = -\frac{\omega R_{LC} C_p}{[1 + \omega^2 R_{LC}^2 (C_p + C_{LC})^2]^{1/2}} U_0 \cos(\omega t + \delta) \quad 3$$

$$\tan\delta = \omega R_{LC} (C_p + C_{LC})$$

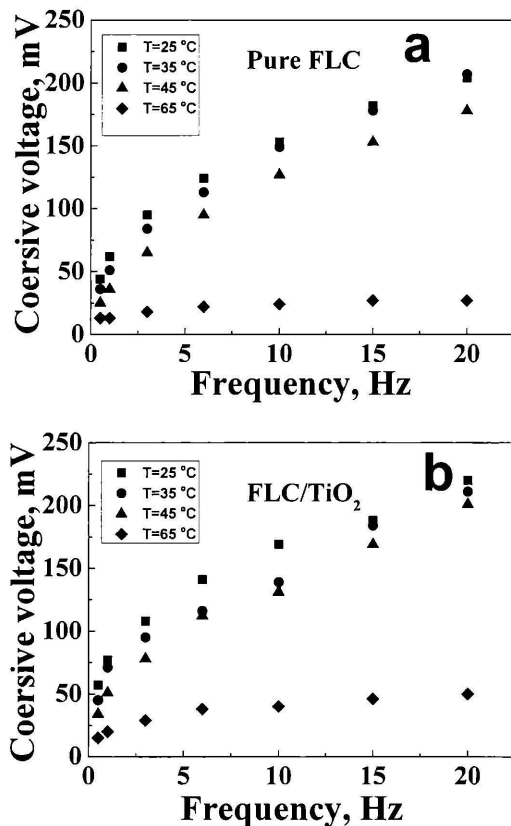


Figure 6: Dependence of the coercive voltage on the frequency for LAHS1 (a) and LAHS1/ TiO₂ nanodispersion (b) on the frequency of the driving triangular-wave voltage. The amplitude of the applied voltage is 10 V ($E=5 \times 10^6$ V/ μ m). Temperatures 25°C, 35°C, 45°C and 65°C.

Here R_{LC} is the resistivity of the cell, C_p and C_{LC} are capacitances of the alignment layers and the FLC layer, respectively. The characteristic time of the voltage divider $\tau_d = R_{LC}(C_p + C_{LC})$ is predetermined, in turn, by the hysteresis inversion frequency f_i . The higher the difference between the frequency of the applied field and $f = 2\pi/\tau_d$ is the higher the coercive voltage should be. In our case, the capacitance of the FLC/TiO₂ cell is different from that of pure FLC. From the combination of the parameters (R_{LC}, C_p, C_{LC}) follows that the cells with nanocomposites shows higher coercive voltage. It means that LAHS1/TiO₂ nanodispersion is suitable for application in bistable spatial light modulators.

Conclusion

It was demonstrated that dispersion of the dielectric TiO₂ nanoparticles in chiral liquid crystals lead to the significant enhancement of their optical, electrooptical and dielectric properties. TiO₂ nanoparticles increase the Goldstone mode relaxation frequency and decrease the dielectric strength of ferroelectric liquid crystals, which can

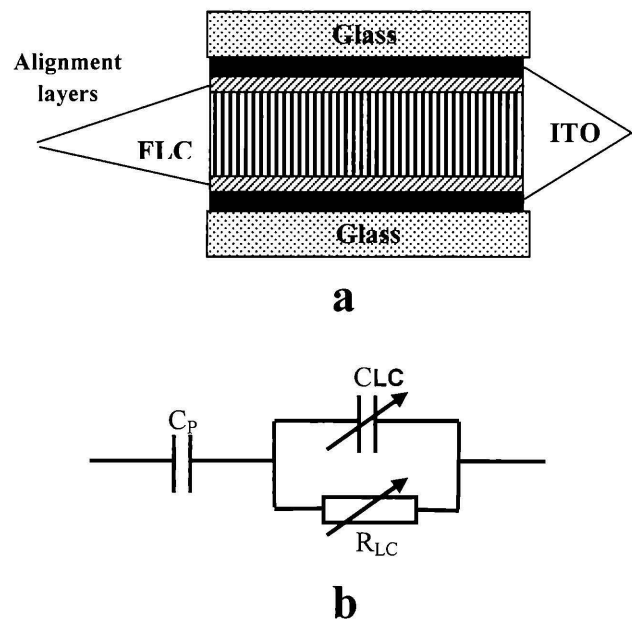


Figure 7: a) Structure of a FLC cell, b) Equivalent electrical circuit of the ferroelectric liquid crystal cell; C_p – capacitance of the alignment layer, C_{LC} – capacitance of the FLC layer, R_{LC} – resistivity of the alignment layer

be explained by the significant decrease of the Frank elastic constant. In the same time, decrease of the dielectric strength results, according to the voltage divider model, as an increase of the coercive voltage of the electrooptical curve (transmission vs applied voltage), which makes the FLC/TiO₂ perspective for application in bistable spatial light modulators.

Dispersion of TiO₂ nanoparticles in cholesteric liquid crystal/laser dye mixture leads to the tremendous modification of the spectrum of the emitted light under excitation of this mixture by Q-switched Nd:YAG laser beam. The appearance of the second lasing peaks can be explained either by the influence of the nanoparticles on the helical pitch of the CLC or due to the topological texture defects induced by the nanoparticles.

Acknowledgements

The authors are thankful to German Federal Ministry for Education and Research (grant BMBF/DLR 08/10) and German Science Foundation (HA 782-98-1). We are also grateful to Dr. A. Lapanik for preparation of LAHS1 FLC mixture and fruitful discussions.

References

- [1] L. M. Blinov, Structure and properties of Liquid Crystals, Dordrecht- Heidelberg- London- New York, Springer Publish.(2011).
- [2] W. de Boer, Active matrix liquid crystal displays, Oxford, Elsevier(2005)
- [3] P. Poulin, H. Stark, T. C. Lubensky, and D. A. Weitz, Science, 275, 1770, (1997).
- [4] H. Stark, A. Borštnik and S. Žumer, Defects in Liquid Crystals: Computer Simulations, Theory and Experiments, NATO Science Series, 43, 37-85, (2002).
- [5] M. Kléman and O. D. Lavrentovich, Soft Matter Physics: an Introduction, New York, Springer Publish. 2003
- [6] O. D. Lavrentovich, I. Lazo, and O. P. Pishnyak, Nature, 467, 947, (2010).
- [7] A. V. Ryzhkova, F. V. Podgornov, and W. Haase, Appl. Phys. Lett., 96, 151901, (2010).
- [8] O. P. Pishnyak, S. V. Shiyankovskii, and O. D. Lavrentovich, Phys. Rev. Lett., 106, 047801, (2011).
- [9] H. Y. Chen and W. Lee, Opt. Rev., 12, 223, (2005).
- [10] H. Y. Chen and W. Lee, Appl. Phys. Lett., 88, 222105, (2006).
- [11] I. Baik, S. Y. Jeon, S. H. Lee, K. A. Park, S. H. Jeong, K. H. An, and Y. H. Lee, Appl. Phys. Lett., 87, 263110, (2005).
- [12] H. Y. Chen and W. Lee, Proc. of SPIE, 5947, 59470T, (2005).
- [13] W. Lee and H. Y. Chen, Jpn. J. Appl. Phys. 46, 5A, 2962, (2007).
- [14] T. Togo, K. Nakayama, M. Ozaki, and K. Yoshino, Jpn. J. Appl. Phys. 36, L1520 (1997).
- [15] S. B. Lee, K. Nakayama, T. Matsui, M. Ozaki, and K. Yoshino, IEEE Transactions on Dielectrics and Electrical Insulation 9, 31 (2002).
- [16] P. Arora, A. Mikulko, F. Podgornov, and W. Haase, Mol. Cryst. Liq. Cryst., 502, 1 (2009).
- [17] F. V. Podgornov, A. V. Lapanik, W. Haase, and A. M. Suvorova, Chem. Phys. Lett., 479, 206 (2009).
- [18] A. Mikulko, P. Arora, A. Glushchenko, A. Lapanik, and W. Haase, Europhys. Lett. 87, 27009, (2009).
- [19] A. Glushchenko, C. I. Cheon, J. West, F. Li, E. Büyüktanir, Y. Reznikov, and A. Buchnev, Mol. Cryst. Liq. Cryst., 453, 227 (2006).
- [20] M. Inam, G. Singh, A. M. Biradar, and D. S. Mehta, AIP Advances 1, 042162 (2011).
- [21] Y. A. Garbovsky and A. V. Glushchenko, Solid State Physics, 62, 1-74, (2011).
- [22] F. V. Podgornov, A. V. Ryzhkova, and W. Haase, Appl. Phys. Lett. 97, 212903, (2010).
- [23] L. M. Blinov and R. Bartolino, Liquid Crystal Microlasers, Transworld Research Network, Kerala, India, (2010).
- [24] M. Mitov, C. Bourgerette, and F. de Guerville, J. Phys.: Cond. Mat., 16, 1981, (2004).
- [25] W. Haase, F. Podgornov, Y. Matsuhisa, and M. Ozaki, Physica Status Solidi A, 204, 3768, (2007).
- [26] P. K. Mandal, S. Haldar, A. Lapanik and W. Haase, Jap. J. Appl. Phys. 48, 011501, (2009)
- [27] L. M. Blinov, E. P. Pozhidaev, F. V. Podgornov, A. Sinha, and W. Haase, Ferroelectrics, 277, 3, (2002).
- [28] S. P. Palto, L. M. Blinov, F. V. Podgornov, and W. Haase, Mol. Cryst. Liq. Cryst., 410, 623, (2004).
- [29] L. M. Blinov, S. P. Palto, E. P. Pozhidaev, F. V. Podgornov, W. Haase, and A. L. Andreev, Mol. Cryst. Liq. Cryst., 410, 633, (2004).